



**HAL**  
open science

## Standardized cross-linking determination methods applied to POE encapsulants in lamination recipe emphasizing

Margot Landa Pliquet, Timea Béjat, Marion Serasset, Axel Descormes, Eeva Mofakhami, Eszter Voroshazi

### ► To cite this version:

Margot Landa Pliquet, Timea Béjat, Marion Serasset, Axel Descormes, Eeva Mofakhami, et al.. Standardized cross-linking determination methods applied to POE encapsulants in lamination recipe emphasizing. EU PVSEC 2023 - 40th European Photovoltaic Solar Energy Conference & Exhibition, Sep 2023, Lisbonne, Portugal. cea-04284516

**HAL Id: cea-04284516**

**<https://cea.hal.science/cea-04284516>**

Submitted on 14 Nov 2023

**HAL** is a multi-disciplinary open access archive for the deposit and dissemination of scientific research documents, whether they are published or not. The documents may come from teaching and research institutions in France or abroad, or from public or private research centers.

L'archive ouverte pluridisciplinaire **HAL**, est destinée au dépôt et à la diffusion de documents scientifiques de niveau recherche, publiés ou non, émanant des établissements d'enseignement et de recherche français ou étrangers, des laboratoires publics ou privés.

# Standardized cross-linking determination methods applied to POE encapsulants in lamination recipe development

Margot Landa - Pliquet <sup>1\*</sup>, Timea Béjat <sup>1</sup>, Marion Serasset <sup>1</sup>, Axel Descormes <sup>1</sup>, Eeva Mofakhami <sup>1</sup>,  
Eszter Voroshazi <sup>1</sup>

<sup>1</sup>Univ. Grenoble Alpes, CEA, Liten, INES, Le Bourget du Lac, France

\*Corresponding author: Margot Landa- Pliquet, [margot.pliquet@cea.fr](mailto:margot.pliquet@cea.fr)

## Abstract

Ethylene vinyl acetate is the most common encapsulation material in photovoltaic panels. Due to gradual engineering, it ensures to meet performance requirements of standard cells, it is low-cost and has well understood cross-linking behaviour, both physically and chemically. Nowadays polyolefin elastomers (POE) have been entering the PV industry to meet the requirements of advanced cells concepts and/or novel degradation phenomena noticed on bifacial modules. POE exhibits several advantages based on its intrinsic high volume resistivity, low permeation, processability and most importantly, the absence of harmful by-products (such as acetic acid) generated upon humidity exposure. However, this new materials family may behave differently from EVA during crosslinking, thus it is necessary to verify and adapt standard measurement methods. Therefore, the main objective of this study is to investigate the cross-linking behaviour of POEs with the final goal of exploring the process window of the lamination. The characterization methods like differential scanning calorimetry (DSC) and Soxhlet extraction have been used to determine crosslinking rate and chemical structure of several POE encapsulants. Similar to EVAs, cross-linking rate of POEs measured by Soxhlet extraction increases with lamination duration until approaching a horizontal asymptote. The indirect cross-linking rate measurement by DSC analysis is usually favoured through its simple and fast implementation, absence of toxic chemicals handling when compared to Soxhlet extraction. In the case of highly engineered materials, clear deviations are recorded, highlighting validity limits of direct correlation between Soxhlet and DSC methods. Nevertheless, we obtained remarkable correlations between these two techniques for two commercially available POEs, allowing the extension of the IEC standard to new encapsulants.

## 1. Introduction

The photovoltaic (PV) industry has experienced remarkable growth as a key player in the global transition towards clean and sustainable energy [1]. PV technology is an increasingly competitive technology owing to its continued performance increase and improvement in durability coupled with mass manufacturing ensuring its low cost. A photovoltaic module typically consists of interconnected solar cells encapsulated in a polymer (encapsulant) to ensure durability and weather resistance, covered on the front side by a glass or transparent cover and at the rear side by a glass or a backsheet for moisture protection and electrical insulation. Understanding the composition and progress in materials used in the PV industry is crucial for optimizing module performance, increasing energy yield, and ensuring long-term durability.

The front glass acts as a transparent barrier, allowing sunlight to pass through while protecting the underlying components from external elements such as moisture, abrasion and mechanical and physical damage. Additionally, the glass cover also acts as a mechanical support, contributing to the overall structural stability of the panel. The backsheet serves as an electrical insulator and a protective layer; its primary function is to prevent moisture ingress, and to act as a barrier against environmental stresses and degradation of the solar cells [2], [3]. The backsheet core material is typically a polymer-based film, such as polyvinyl fluoride (PVF), polyethylene terephthalate (PET), or polyamides (PA) [4].

The encapsulant plays a crucial role in the composition of a solar panel. It acts as a protective layer, preventing moisture ingress, mechanical damage, and environmental degradation. Ensuring the long-term reliability and performance of PV modules necessitates effective encapsulation materials that shield the solar cells from environmental factors and ensure adherence to solar cells and cover layers [5]. Ethylene-vinyl acetate copolymer (EVA) is traditionally used as an encapsulant due to its excellent cost-performance balance, more precisely its transparency, flexibility, easy handling, high transparency, good optical and mechanical properties and over 35 years of field experience [6], [7]. Solar-grade EVA is a semi-crystalline random copolymer of ethylene and vinyl acetate, with a vinyl acetate content ranging from 28 to 33% [8]. To ensure thermal and thermo-mechanical stability, the material contains curing agents (peroxides) that enable chemical crosslinking during the lamination process [9]. This process forms a three-dimensional polymer network. Silanes compounds are also incorporated in the formulation to improve adhesion to glass and UV stabilizers to protect against degradation.

However, EVA has some limitations in terms of durability driving to power losses and reduced module performances:

- Yellowing: Over time, EVA can undergo yellowing, leading to a reduction in the transparency of the encapsulant. This can decrease the amount of light reaching the solar cells, reducing power output [10], [11].
- Degradation: The chemical degradation of EVA leads to the production of acetic acid (undesired by-product), which remains in the PV module due to the impermeability of the adjacent layers. The presence of acetic acid can cause corrosion of interconnections or potential-induced degradation (PID) when acetic acid promotes the migration of sodium ions from front glass to solar cells [12]. The chemical mechanism of EVA thermal degradation was firstly highlighted by Allen *et al.* [13]
- Delamination: EVA may be susceptible to delamination from other components of the PV module. Delamination can occur due to factors such as temperature variations, moisture ingress, and mechanical stress, compromising the integrity of the module [14], [15].

The demand for improved module efficiency, longer lifespan, and enhanced reliability necessitates the development of new encapsulation materials that offer better resistance to environmental stressors, improved adhesion, higher transparency, and advanced moisture barrier properties. Exploring alternative encapsulation materials is crucial to meet the evolving needs of the solar industry and maximize the potential of photovoltaic technology. Over the past decade, research and development efforts have been devoted to exploring alternative materials to replace traditional EVA as encapsulants for solar cells. This attempt has led to the emergence of several promising materials in this field. Polyolefin elastomer (POE) encapsulants have gained popularity and are now commonly used commercially. These materials are polyethylene-based and require the use of curing agents for cross-linking, similar to EVA. The POE encapsulants offer notable advantages, including superior volume resistivity and reduced permeability to moisture and sodium ions within the module [16]. These properties significantly contribute to mitigate the risks of potential-induced degradation (PID) and transmittance loss [17]–[19]. In recent years, there has been a rise in the introduction of novel encapsulation materials that align with the progress in solar cell technologies. This category includes thermoplastic polyolefin (TPO) [20], [21], polyvinylbutyral (PVB) [22], ionomers [23], [24] and multi-layer encapsulants such as EPE [25]. These new encapsulation materials show promising characteristics, such as improved performance, enhanced reliability, and reduced degradation rates,

paving the way for the improvement of more efficient and durable solar cell modules [26]. Raw material price evolution is also an important innovation driver, where POE encapsulants need enhancement [27].

The industrial manufacturing process for solar panels is based on a hot vacuum lamination process. First, the interconnected solar cells and other components are stacked and carefully aligned. Then, the assembly passes through a laminator, where heat and pressure are applied with a vacuum stage in the process. During this step, the encapsulants melt, allowing the layers to bond together, which is essential for the crosslinking of the encapsulants. The lamination temperature is chosen to be higher than the peroxide decomposition temperature to achieve correct crosslinking. Furthermore, silane promoters create covalent bonds to the encapsulants and the silicate moieties of the glass during the curing process. To optimize the lamination process, control measurements like temperature monitoring, pressure regulation and crosslinking rate evaluation of the encapsulant are implemented. It is crucial to have a correct crosslinking rate to ensure the required thermo-mechanical polymer properties crucial for long-term durability of the module.

There are various techniques available for measuring the degree of cure of encapsulant materials, some adaptable to industrial production some remaining at laboratory level. These methods help assessing the extent of chemical crosslinking. The Soxhlet extraction method involves extracting the soluble fraction of the encapsulant and quantifying the weight percentage of the insoluble gel fraction, providing a quantitative assessment [28], [29]. However, this method requires the use of hazardous chemicals and is time-consuming, making it unsuitable for rapid quality control [30]. DMA (Dynamic Mechanical Analysis) measures the mechanical response of PV encapsulants under controlled oscillatory stress or strain, evaluating parameters such as storage modulus ( $E'$ ), loss modulus ( $E''$ ), and damping factor ( $\tan \delta$ ) to quantify the crosslinking degree [31], [32]. This method is also destructive and time-consuming and necessitate a good calibration step to produce pertinent results. Differential Scanning Calorimetry (DSC) measures heat flow during heating and cooling cycles, providing information on peroxides decomposition reactions and melting/crystallization peaks, which indirectly indicate the crosslinking degree [33], [34]. Fourier Transform Infrared Spectroscopy (FTIR) analyses the infrared absorption spectrum before and after curing, enabling determination of the crosslinking degree by examining specific absorption peaks associated with crosslinking functional groups [28], [34]. Some authors have obtained clear correlations on crosslinking rate values obtained by these techniques for EVA [28], [29]. An alternative fast and non destructive method is indirect correlation of EVA crosslinking to its viscoelastic properties as presented by LayTec which can be used as an inline process control [35]. Nevertheless, there is a need to verify these cross correlations for new advanced encapsulants like POEs. As of our current understanding, there are no existing publications available on this particular topic.

The aim of this paper is to apply standardized cross-linking ratio determination method to commercially available POE encapsulants [36], [37], with the goal of enhancing the development of lamination recipes. An essential aspect of optimizing the lamination process is to achieve a balance between pressure, temperature, and duration to obtain the most reliable, durable and cost-effective PV modules. Throughout this optimization process, several tests are recommended to verify the degree of cross-linking and the amount of remaining peroxides within the modules. Indeed, the first objective of this investigation is to assist lamination process development by validating the implementation of fast but indirect DSC measurement for POEs, and by identifying a process window with limited duration and thus accelerate the integration of this novel encapsulant in innovative PV modules. The second objective is to identify the limitations of the current version of the IEC62788-1-6 standard on crosslinking rate measurement for a reproducible study of POE encapsulants and suggest some adaptations in the protocol.

## 2. Experimental part

### 2.1. Lamination process of studied encapsulants

The experimental plan of this study includes three materials: an ethylene-vinyl acetate (EVA) and two polyolefin elastomer (POE) encapsulants, all commercially available. Each time we had several samples from each lamination recipe. The lamination was conducted on commercial hot vacuum laminator with membrane enabling pressure on sample without surrounding air.

We varied two parameters: the lamination temperature and the lamination pressure duration for each material. Lamination recipes have been developed at three different temperatures: 150, 160 and 170 °C for lamination times ranging from 5 to 30 minutes.

Hot vacuum lamination process needs special sample preparation, identical to industrial PV module manufacturing. As a first step, lamination recipe should be developed according to the used bill of materials (BOM). To reproduce real PV module configuration we placed uncured encapsulant sheets between two solar glasses separated by PTFE liners to enable separation after lamination to extract encapsulant film only, as presented in Figure 1. This stack was placed in the laminator, then we launched a standard lamination cycle to obtain samples for Soxhlet extraction study or for DSC analysis according to required lamination temperature and duration.

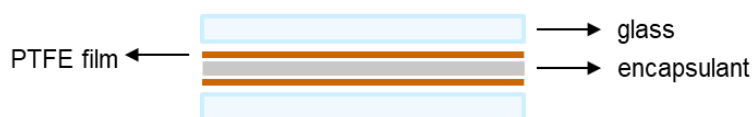


Figure 1. Lamination stack for sample preparation

### 2.2. Sample preparation

From laminated sheets of each encapsulants, we proceed to extract the desired sized samples. As studied encapsulants' thickness was variable, we targeted a constant mass (1 g) instead of a constant area for all samples. From each encapsulant, we obtained two samples for Soxhlet extraction and two samples for DSC analysis. We assured a repeatability of all results this way.

### 2.3. Differential scanning calorimetry

We used a differential scanning calorimetry (DSC) instrument, specifically the TA Waters Q20 model, for conducting material thermal analysis. The apparatus uses a reference empty capsule, and a sample-filled one to analyze the difference between heat fluxes across each capsule's bottom surface. To prepare the launch of this analysis, we used aluminium hermetic pans and lids, closed by a crimper supplied by the machine manufacturer. The samples weighed between three and six milligrams and all measurements were carried out under a continuous nitrogen flow to prevent oxidation. The DSC measurement procedure involved three steps. First, a heating scan from 40 °C to 100 °C at a thermal rate of 10 °C/min was performed to eliminate the thermal history of our samples. Subsequently, a cooling step from 100 °C to -20 °C was achieved at the same rate to reveal the recrystallization region. Finally, a second heating scan from -20 °C to 250 °C was executed at 10 °C/min to observe both the melting and the curing agent decomposition regions. A typical DSC thermogram displayed in Figure 2, illustrates the results of the analysis.

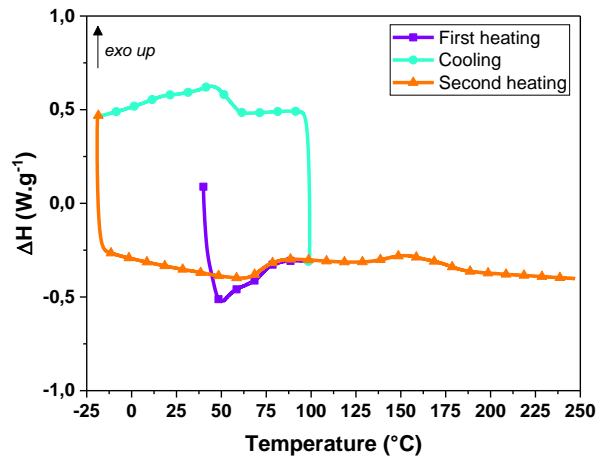


Figure 2. Typical DSC thermogram

DSC analysis enables to calculate the crosslinking rate of a laminated solar encapsulant according to IEC62788 standard [37]. This standard presents two calculating methods within the DSC methodology: the residual enthalpy method (RE) (Figure 3) and the Melt-Freeze method (MF) (Figure 4). The residual enthalpy method by DSC consists in using the enthalpy of uncured sample ( $H_u$ ), considered as 100% charged in peroxides and the sample under study ( $H_t$ ) where we are looking for the remaining peroxide rate after lamination (Equation 1).

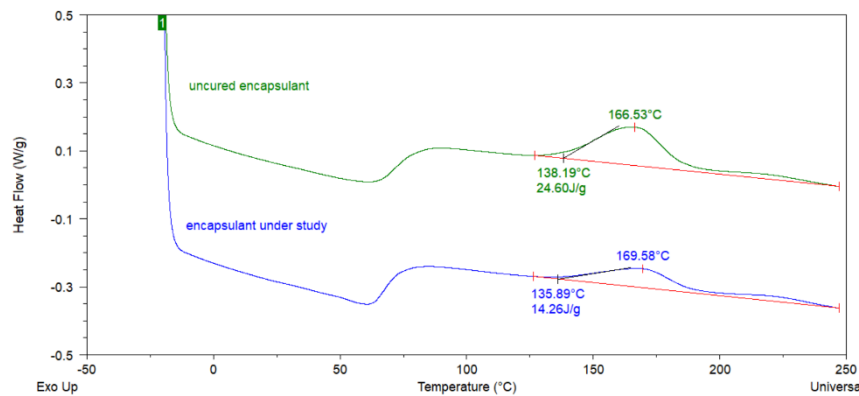


Figure 3. DSC methodology to determine crosslinking rate by RE method

$$G_e = \frac{H_u - H_t}{H_u} \times 100 \quad \text{Equation 1}$$

Hidalgo *et al.* [38] presented the melt/freeze method of the standard. This method requires crystallization peak ( $T_c$ ) and onset ( $T_o$ ) temperatures determination as well as the shape factor ( $SF$ ) of the thermogram. With this data, the cross-linking rate is calculated (Equation 2). As described by Hidalgo *et al.*, an automated algorithm was developed in-house to integrate the method and calculate the cross-linking rate independently from EVA's intrinsic parameters.

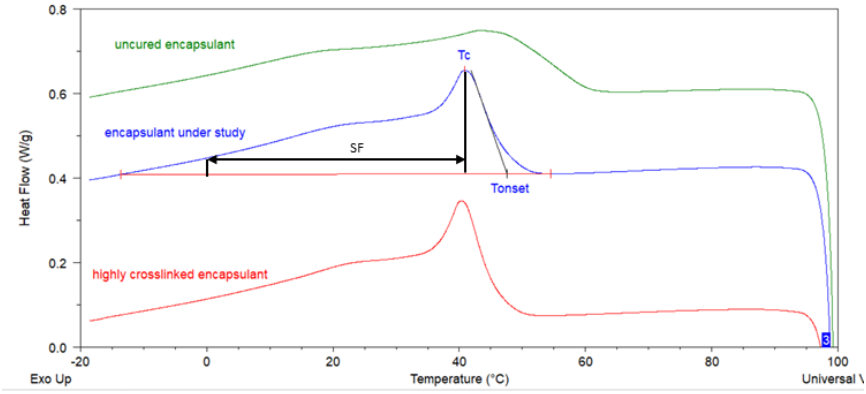


Figure 4. DSC methodology to determine crosslinking rate by Melt/Freeze method

$$G_a = \left( \frac{T_c + T_o + SF}{3} \right) \quad \text{Equation 2}$$

IEC62788 standard [40] details completely both methods with clear graphical representation of each required quantity, readers may refer to this document for further information.

#### 2.4. Soxhlet extraction

We used a four-column Soxhlet extractor (100 mL) with 250 mL balloons for this study. The solvent was toluene and we used water as refrigerating liquid in a closed loop. Figure 5 presents our experimental installation. For thimble drying, a small (30 L) laboratory oven was used while for gravimetric analysis a Sartorius  $10^{-3}$  Gramm precision balance served for weighing samples before and after extraction. The gel content was calculated by Equation 3:

$$X_{gel}(\%) = \frac{m_{final(sample)}}{m_{initial(sample)}} \quad \text{Equation 3}$$

In the formula,  $X_{gel}$  represents the cross-linked gel content,  $m_{final(sample)}$ , the final mass of the encapsulation specimen after drying and  $m_{initial(sample)}$ , the initial mass of the encapsulation specimen before extraction.



Figure 5 Multi-column Soxhlet extractor installation at laboratory

Each stage of Soxhlet extraction (thimble drying temperature and duration, extraction time, sample mass) underwent optimisation to match best performance with shortest process time.

### 2.5. Infrared spectroscopy

We used a Thermo Scientific Nicolet 6700 FT-IR to record FTIR spectra with ATR (attenuated total reflectance) measuring accessory. We recorded first a background measurement that serves to correct recorded experimental data, and then all studied encapsulants were placed under the diamond crystal for the ATR measurements. A total number of 32 scans and a resolution of  $4\text{ cm}^{-1}$  within the spectral range of  $4000$  to  $525\text{ cm}^{-1}$  were recorded.

We analyzed measured data by OMNIC software for element identification and displayed data by ORIGIN Pro 2020 software.

## 3. Results

### 3.1. DSC analysis

The thermal properties of the three encapsulants in our study were examined. Figure 6 illustrates the DSC thermograms of the uncured encapsulants. Three thermal phenomena occur during a typical DSC analysis. First, during the heating run, the encapsulants melt over a wide melting range between  $40$  and  $80\text{ }^{\circ}\text{C}$ . POEs show a melting peak at  $60\text{ }^{\circ}\text{C}$  while the EVA encapsulant melts rather at  $70\text{ }^{\circ}\text{C}$ . Then at higher temperatures, a significant exothermic peak appears around  $160\text{ }^{\circ}\text{C}$  indicating the thermal decomposition of the crosslinking agent (peroxide type), and simultaneously the crosslinking reaction of the encapsulants. The DSC curves of POE 1 and EVA display a similar shape, suggesting that the peroxide species used seem to be identical. However, the DSC curve of the POE 2 encapsulant exhibits two exothermic peaks at  $165\text{ }^{\circ}\text{C}$  and  $195\text{ }^{\circ}\text{C}$ , indicating the possible use of two different types of peroxides as co-curing agents. Finally during the cooling step, a crystallization phenomenon occurs, indicated by an exothermic peak between  $40\text{ }^{\circ}\text{C}$  and  $60\text{ }^{\circ}\text{C}$  depending of the encapsulants; approximately  $50\text{ }^{\circ}\text{C}$  for EVA, whereas POEs crystallize at  $40\text{ }^{\circ}\text{C}$ . In particular, the thermogram of POE 1 shows a significantly broader crystallization peak compared to the other encapsulants. The shape and temperature of the crystallization peak primarily depend of the chemical composition of the encapsulants (vinyl acetate or octene content). Indeed, only the polyethylene part of encapsulants is

involved in melting/crystallization phenomena and the copolymer composition can disturb the PE crystallinity [39].

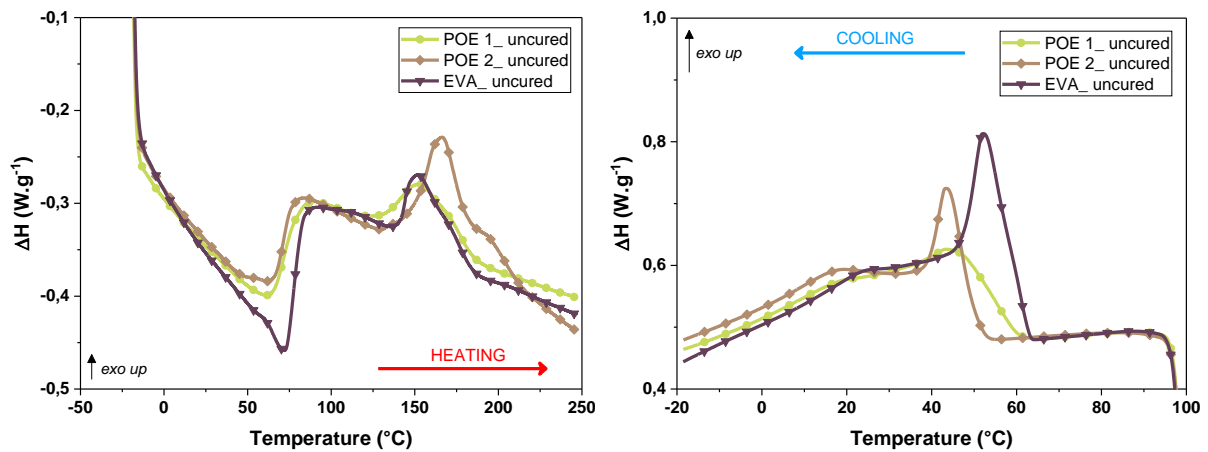


Figure 6. DSC thermograms of the three uncured encapsulants : left) heating run; right) cooling run

We measured each sample of the POE 2 laminated for different durations ranging from 6 to 30 minutes at 150 °C. The outcomes of the variously cured samples are presented in Figure 7. We noticed a shift of the crystallization peak towards lower temperatures. Specifically, between the uncured sample and the sample laminated for 30 minutes at 150 °C, which is considered maximum cured, we observed a shift of approximately 8 °C. Furthermore, the peak's shape is also altered with the increase in crosslinking, leading to narrowing of the crystallization interval. The Melt-Freeze method developed by Hidalgo *et al.* considers three parameters, which describe the evolution of the crystallization peak and determine a crosslinking rate [38], [40]. The  $T_c$  corresponding to crystallization peak temperature, the  $T_{onset}$  when crystallization starts and SF, which is a peak shape factor. Figure 8 shows the resultant crosslinking rate (XL) obtained with the Melt-Freeze method.

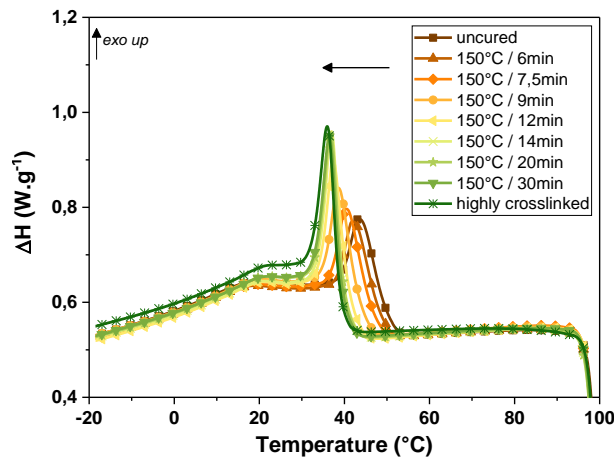


Figure 7. DSC curves of POE 2 samples cured at 150 °C for different durations (cooling step)

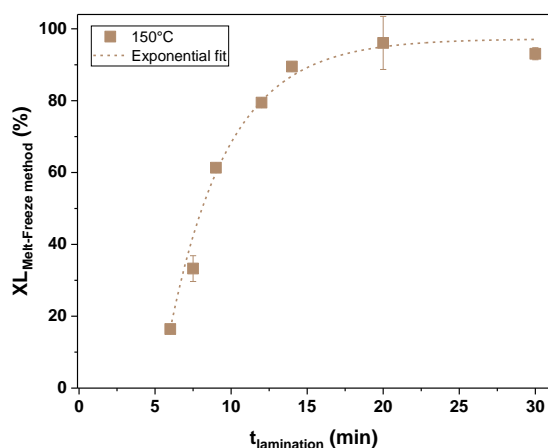


Figure 8. Crosslinking rate (XL) of POE 2 obtained by DSC met-freeze method, case of lamination at 150 °C

A second method, also developed by Hidalgo *et al.*, known as Residual Enthalpy (RE) method, uses the enthalpy of peroxides' decomposition reaction as a parameter to follow for the crosslinking reaction study [38], [40]. The DSC curves corresponding to the uncured and laminated samples of POE 2 during the heating run are presented in Figure 9. The curves were adjusted using Origin software, integrating with a linear baseline. The uncured POE 2 presents a maximal enthalpy of  $12.5 \text{ J.g}^{-1}$  coming from the thermal decomposition of the total amount of curing agent contained in the encapsulation film. For laminated samples, the exothermic peak corresponds to the thermal decomposition of peroxides that have not reacted during lamination stage. Ideally, the residual enthalpy of a fully crosslinked sample should be equal to zero but in certain cases, encapsulant manufacturers add an excess amount of peroxides to the material to ensure that there is sufficient remaining of peroxides for full crosslinking. As the lamination time increases, the peroxides have a longer period for thermal decomposition to initiate the crosslinking reaction. Consequently, the percentage of residual peroxides decreases significantly with the lamination time, as shown in Figure 10. A sharp drop in the exothermic peak occurs quickly showing that curing agents are rapidly consumed during the lamination stage (around 6 minutes) but the total reaction of the whole amount of peroxides only takes place for lamination processes lasting 20 minutes at 150 °C or more.

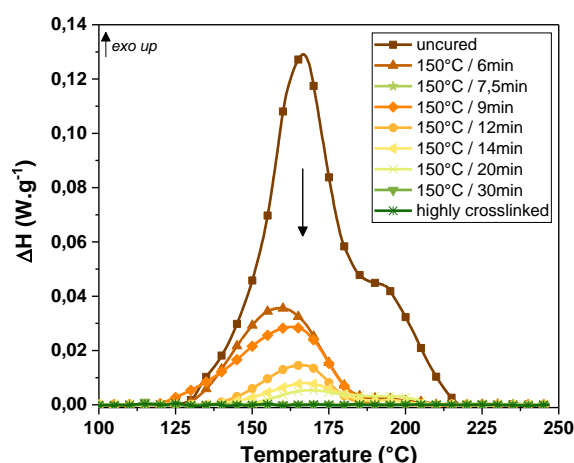


Figure 9. DSC curves of POE 2 samples cured at 150 °C for different durations (heating step)

As the crosslinking agents are typically present in excess in the material, the method of assessing the crosslinking degree based on residual enthalpy method may be subject to errors [40]. In fact, a fully crosslinked sample (measured by Soxhlet and DSC melt/freezing method) might still contain a non-

negligible amount of so-called residual peroxides. Consequently, the residual peroxides content may continue to decrease until it reaches zero, while the crosslinking degree is stabilized at its maximum level.

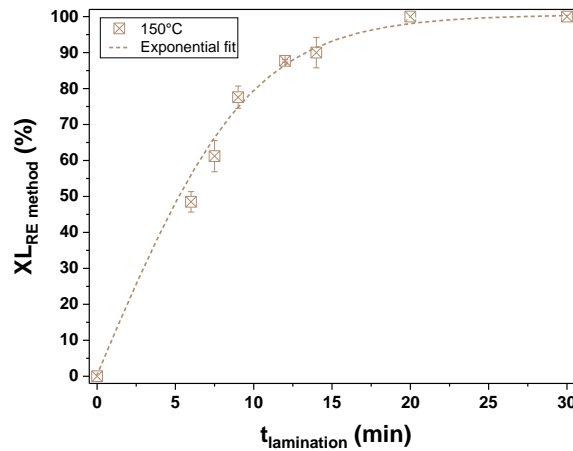


Figure 10. Crosslinking rate (XL) of POE 2 obtained by DSC RE method, case of lamination at 150 °C

The POE 1 encapsulant was studied at three lamination temperatures: 150, 160 and 170 °C and for several durations. The resultant crosslinking rate evolution obtained by the Melt/Freeze method is displayed in Figure 11. The results show a strong time dependence at the beginning of the experiment followed by an inflection towards high XL values after about ten minutes, depending of the process temperature. In this case, POE 1 exhibits gel contents of up to 80%, and this maximum level is achieved regardless of the lamination temperature; it only requires more or less time.

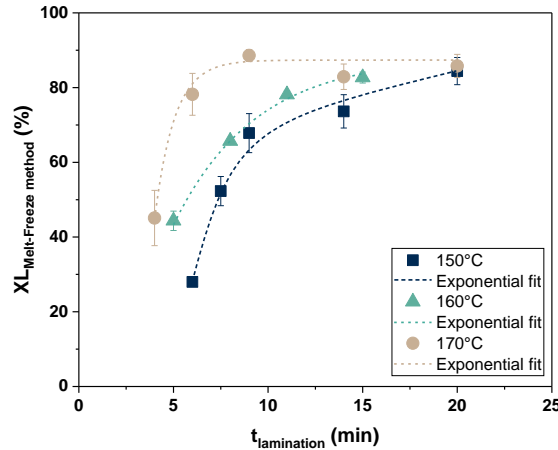


Figure 11. Crosslinking rates (XL) of POE 1 at three different temperatures

### 3.2. Soxhlet extraction

The insoluble content of each encapsulant was determined using the Soxhlet extraction method, and the resultant crosslinking rate was calculated following Equation 3. The data is plotted in Figure 12. The investigated samples were laminated for durations ranging from 4 to 30 minutes at process temperatures varying between 150°C and 170°C. From plotted graphs, it is clearly visible that crosslinking phenomenon was initiated rapidly. Independently of the type of encapsulant used, a sharp increase in the cross-linking rate occurred during short lamination times, which later seemed to stabilize. The three materials selected for this study are classified as fast and very fast cured encapsulants, as they achieve their recommended cross-linking rate in less than 10 minutes. By

elevating the temperature during the lamination process, the fast crosslinking phenomenon can be intensified, leading to an increased production rate of PV modules. A reduction in manufacturing time from 25 minutes to approximately ten minutes can be achieved.

Soxhlet extraction is a particularly well suited characterization technique for determining the cross-linking rate of polymer materials. This technique yields reliable and quantitatively accurate values compared to indirect methods such as DSC or FTIR spectroscopy. It is particularly suitable for materials with a cross-linking rate exceeding 50%, which is the case for PV encapsulants. However, it may produce results with higher uncertainties for materials exhibiting low crosslinking rates. In such cases, an increased number of free polymer chains need to be extracted. Throughout our study, each data point represents a minimum of two separate measurements. Although there were some uncertainties associated with samples with cross-linking rates below 40%, the majority of our measurements delivered highly reliable results, with a relative error of less than 1%. The maximum cross-linking rate measured by this method is 75% for POE samples and 89% for EVA. Even with significantly extended lamination times, certain portions of the material remain soluble, indicating the presence of uncrosslinked polymer chain fragments and various additives (such as UV absorbers, antioxidants, etc.).

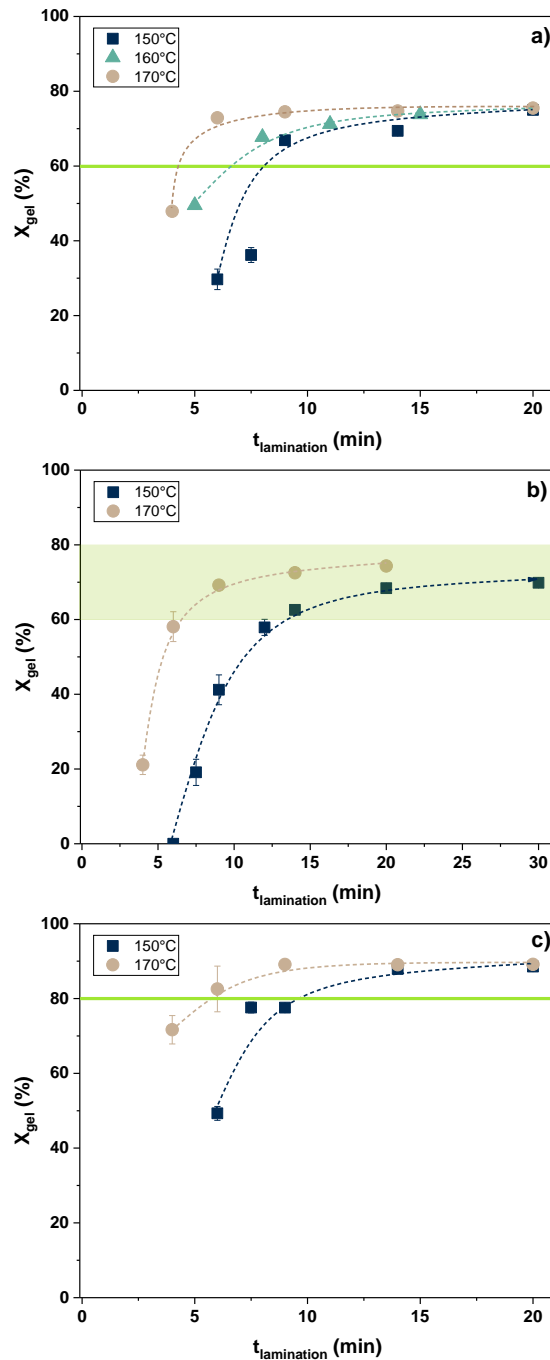


Figure 12. Degree of crosslinking measured by Soxhlet ( $X_{gel}$ ) for different curing times and temperatures. a) POE 1; b) POE 2; c) EVA

According to encapsulant supplier's guidelines, it is essential to attain a minimum crosslinking rate of 60% or 80% in the POEs and EVA encapsulants respectively, to meet the necessary mechanical, optical and barrier properties once integrated into a PV module. With these findings (Figure 12), module manufacturers can establish an optimal lamination process to achieve the recommended crosslinking level efficiently.

### 3.3. FTIR spectroscopy

Figure 13 displays the FTIR-ATR spectra of the three encapsulants under investigation recorded in the wavenumber range of 4000 and 600  $\text{cm}^{-1}$ . These obtained results identify our materials as polyolefin and ethylene vinyl acetate copolymers respectively. The three spectra exhibit distinct absorbance

bands that are characteristic of polyethylene including aliphatic CH<sub>2</sub> stretching vibrations at 2915 and 2850 cm<sup>-1</sup>, bending vibrations at 1500 and 1400 cm<sup>-1</sup> [41], [42]. Additionally for the Figure 13.c, we observed specific bands associated with the vinyl acetate copolymer at wavenumbers 1735 cm<sup>-1</sup> (C=O stretching), 1370 cm<sup>-1</sup> (CH<sub>3</sub> bending) and 1236 cm<sup>-1</sup> (CO(=O) stretching) [21]. In comparison, POEs also exhibit a peak at approximately 1700 cm<sup>-1</sup> but with a smaller amplitude than the one observed in EVA. This minor peak in POEs was identified by Wallner *et al.* [32] as a co-curing agent. Additionally, they identified pronounced peaks at 1790, 1720 and 1090 cm<sup>-1</sup> which were attributed to the fast-curing crosslinking agent, stabilizer and silane adhesion promoter. It is crucial to note that these three peaks are not present in the FTIR spectra of our POEs encapsulants. This difference in results compared to Wallner *et al.* [32] can be explained by the fact that their measurement is conducted using FTIR in transmission mode while ours is performed in ATR mode. ATR is limited to probing the near-surface region, and thus, deeper components may not be fully captured in the spectra. Indeed, additives such as crosslinking agents, stabilizers etc. are inhomogeneously distributed throughout the entire film, and it is probable that they were not detected during our ATR measurement.

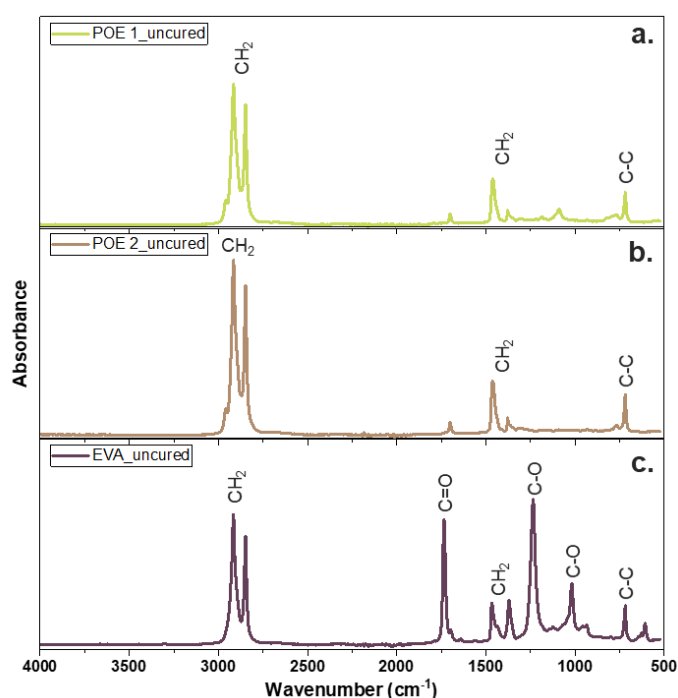


Figure 13. FTIR spectra of uncured POEs and EVA encapsulants

FTIR spectra of the investigated EVA and POE films in the uncured and the fully crosslinked state are illustrated in Figure 14. The crosslinking of the two encapsulants results in a modification of the infrared spectrum, as can be observed in the highlighted regions of the graph. In the case of POE 2, a shift and slight narrowing of the peak at 1700 cm<sup>-1</sup>, attributed to the crosslinking co-agent [36], are observed. Considering that this sample is extensively cross-linked, having undergone lamination for 20 minutes at 170°C, and does not exhibit a peroxide decomposition peak in DSC, it seems highly unlikely that any crosslinking co-agents remain in our case. Then, we noted a reduction in intensity for the shoulder at 1410 cm<sup>-1</sup> and a complete disappearance of the peak at 930 cm<sup>-1</sup>. These bands are commonly associated, respectively, with peroxide-type crosslinker and its co-agent [43]. For the EVA sample, there was an absence of the shoulder at 1789 cm<sup>-1</sup> and 1150 cm<sup>-1</sup>, along with a decrease in intensity for the minor peak at 1695 cm<sup>-1</sup>. In scientific literature, organic peroxides have received limited investigations by spectroscopic techniques, primarily due to the widely accepted notion that the O-O stretching vibration lacks reliable infrared activity [44].

In summary, FTIR analysis highlights changes in the chemical structure due to the encapsulants' crosslinking. However, these differences are mostly subtle and exclusively evident in weak absorbance bands, making this technique challenging to adapt for a kinetic monitoring of crosslinking processes.

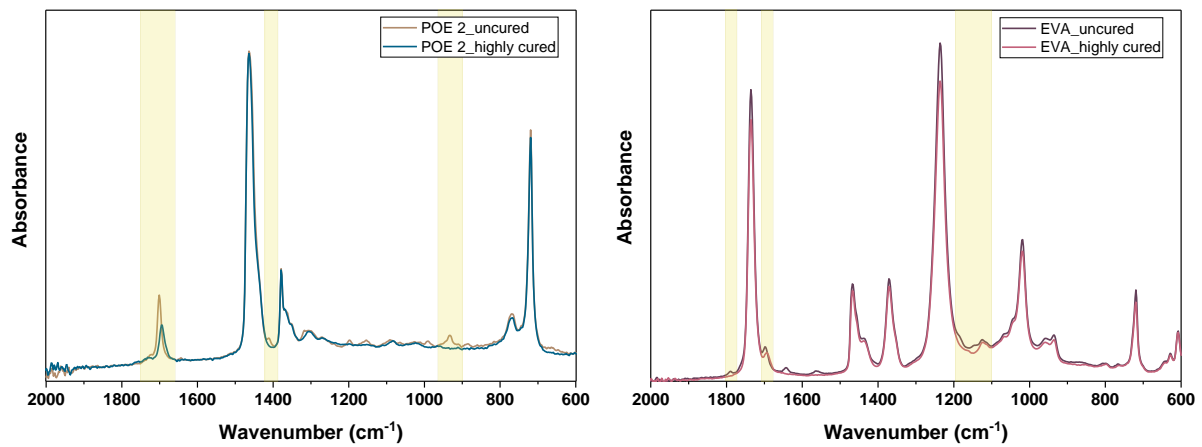


Figure 14. Zoom of the ATR-FTIR spectra of uncured and highly cured encapsulants; left) POE 2, right) EVA

## 4. Discussion

The three presented methods of this paper allow measure crosslinking rate of solar encapsulant films under various lamination conditions. However, the quality and required time to collect data may vary upon the chosen method. To find the optimum between spent time and data quality, we undertook a correlation between our various datasets. Figure 15 displays gel content plotted against crosslinking rate (Melt-Freeze method) obtained for POE 2 encapsulant at two lamination temperatures. A linear correlation was plotted on the figure to demonstrate the excellent alignment of dataset upon a straight line. A previous study tried to dress the same kind of chart for EVA [45]. They fixed the boundary conditions as both methods ran through the zero and the 100% points. This induced a shift from the linear correlation. In our case (Figure 15), the linear correlation line does not run through the point (0;0). Physically, it means that, in encapsulant material, Soxhlet extractor gives a zero level of gel content while the DSC method detects already approximately 15% of cross-linking rate. It may come from the fact that DSC method is a relative method using uncured and maximum cured samples to iterate the studied sample's cross-linking level between these boundary conditions. Physically, a laminated sample could not have zero crosslinking ratio obtained by this method. DSC method compared to Soxhlet extractor method's results shows a systematic overestimation of the crosslinking ratio. We do not recommend using it without a first phase of calibration with Soxhlet extraction to establish a material specific correlation chart as presented in Figure 15.

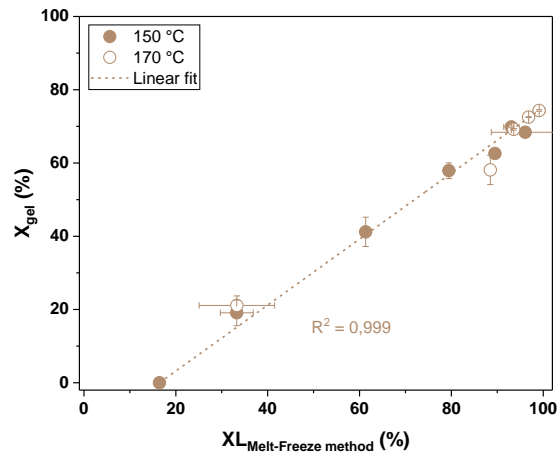


Figure 15. Correlation between DSC and Soxhlet extractor methods for POE 2 at 150 °C and 170 °C lamination temperatures

An excellent correlation between gel content results and DSC crosslinking rates is noticeable in Figure 16 for all our studied samples and for both Melt-Freeze and Residual enthalpy DSC methods. Straight correlation lines were obtained between both techniques, putting in evidence that DSC is an accurate method to determine the crosslinking ratio rapidly and properly. Moreover, this technique is easily implementable as a quality control in PV production line, and do not require the use of hazardous chemical products. Operators do not need special qualification for DSC measurements while for Soxhlet extractor experiments, chemical engineering skills are mandatory to avoid human harm.

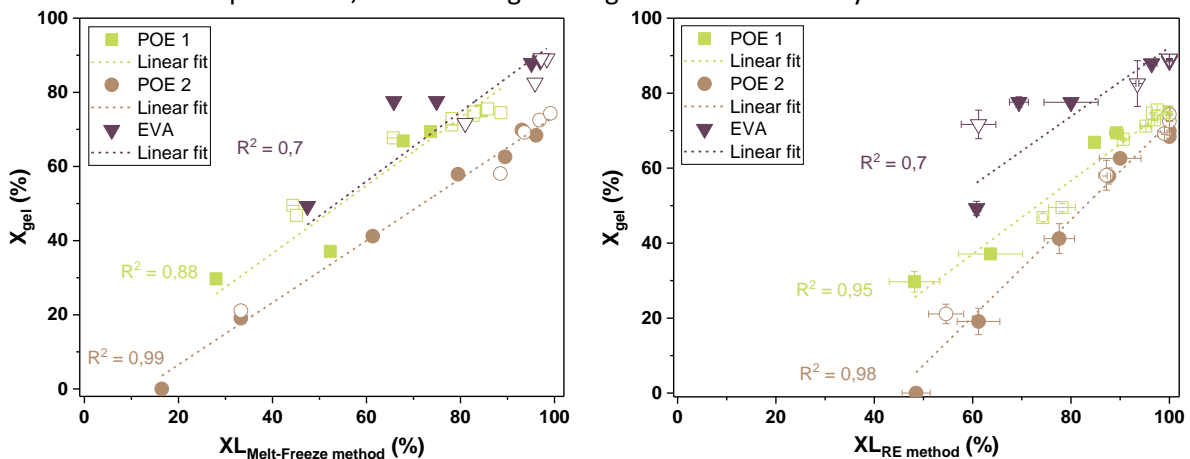


Figure 16. Correlation between DSC and Soxhlet extractor methods for all studied encapsulants at several lamination temperatures

In Figure 16, one can notice that for shorter lamination times, a discrepancy is present between the two methods. The worst case belongs to EVA as this material crosslinks rather quickly, thus even in short lamination duration we obtained very high cross-linking rates giving a cloud of dots mostly in the right region of the chart (values between 80-100%). This gives a broad spread of results within the left part of the chart and make difficult to establish a reliable correlation for shorter lamination times. For this encapsulant, it may be necessary to extend the Soxhlet extraction duration, as it requires more time to extract short polymer chains within a densely crosslinked matrix. POE 2 encapsulant enabled to obtain the highest linear regression that may be explained by the very slow crosslinking kinetics of this material. As we can observe in Figure 15, the correlation lines differ depending on the studied material and the DSC measurement method. It can be noticed that the two POEs (Polyolefin Elastomers) do not follow the same trend; POE 1 approaches the behavior of EVA (Ethylene Vinyl

Acetate). Therefore, it is crucial to verify the crosslinking kinetics for each new material and not assume that all POEs exhibit identical behavior.

## 5. Conclusion

A thorough analysis of cross-linking phenomenon on three commercially available encapsulants had been presented in this study. The applied set of measurement techniques is capable of following the crosslinking effect in two distinct families of encapsulants (POEs and EVA). These methods were compared to the reference method, which is the measurement of gel content using Soxhlet extraction. The DSC residual enthalpy method demonstrated good agreement with the crosslinking rate obtained by Soxhlet extraction, but it is mainly influenced by the quantity of curing additives added to the material by manufacturers. The presented work shows that the previously developed DSC Melt-Freeze method for EVA encapsulants also yields accurate qualitative results for POE encapsulants. The DSC technique offers significant advantages, such as rapid and easy implementation as a quality control measurement, without requiring the use of hazardous chemicals. However, it is important to note that this method provides only an indirect measure of the degree of crosslinking in the sample and needs to be corrected using correlation lines to obtain quantitative values comparable to those obtained by Soxhlet extraction. FTIR spectroscopy was used to identify the three encapsulants as POEs and EVA encapsulants. Since the crosslinking effect is not easily visible in the infrared spectra, caution is advised when using this technique to monitor crosslinking kinetics. Furthermore, the results obtained confirm that correlation lines are dependent on the specific material formulation and must be developed for each encapsulant. Therefore, introducing new materials in PV modules and development, control of the lamination process should be preceded by detailed characterization to ensure successful implementation. This investigation emphasizes the importance of characterizing the crosslinking of the encapsulant in order to assess the quality of industrially produced modules.

For further investigation, it would be beneficial to complement this study by characterizing other existing POEs available in the market. Furthermore, to avoid measurement errors at low and high crosslinking levels, we recommend extending the Soxhlet extraction time suggested in the current version of the IEC standard to at least 24 hours, allowing all free polymer chains to be thoroughly extracted.

## Acknowledgements

Authors would like to thank Amandine Boulanger for valuable help with lamination process development. The authors would also like to recognize the technical contribution of the 3SUN module team as well as funding from INES2S.

## References

- [1] V. Masson-Delmotte *et al.*, « IPCC, 2018: Global Warming of 1.5°C », An IPCC Special Report on the impacts of global warming of 1.5°C above pre-industrial levels and related global greenhouse gas emission pathways, in the context of strengthening the global response to the threat of climate change, sustainable development, and efforts to eradicate poverty. [https://www.ipcc.ch/site/assets/uploads/sites/2/2019/06/SR15\\_Full\\_Report\\_Low\\_Res.pdf](https://www.ipcc.ch/site/assets/uploads/sites/2/2019/06/SR15_Full_Report_Low_Res.pdf)
- [2] A. Omazic *et al.*, « Increased reliability of modified polyolefin backsheets over commonly used polyester backsheets for crystalline PV modules », *Journal of Applied Polymer Science*, vol. 137, n° 30, 2020, doi: [10.1002/app.48899](https://doi.org/10.1002/app.48899).

- [3] J.-W. Zhang *et al.*, « Aging phenomena of backsheet materials of photovoltaic systems for future zero-carbon energy and the improvement pathway », *Journal of Materials Science & Technology*, vol. 153, p. 106-119, 2023, doi: [10.1016/j.jmst.2022.12.063](https://doi.org/10.1016/j.jmst.2022.12.063).
- [4] K. J. Geretschläger *et al.*, « Structure and basic properties of photovoltaic module backsheet films », *Solar Energy Materials and Solar Cells*, vol. 144, p. 451-456, 2016, doi: [10.1016/j.solmat.2015.09.060](https://doi.org/10.1016/j.solmat.2015.09.060).
- [5] M. Kempe, « Encapsulant Materials for PV Modules », in *Photovoltaic Solar Energy*, John Wiley & Sons, Ltd, 2016, p. 478-490. doi: [10.1002/9781118927496.ch43](https://doi.org/10.1002/9781118927496.ch43).
- [6] S. Jiang *et al.*, « Encapsulation of PV Modules Using Ethylene Vinyl Acetate Copolymer as the Encapsulant », *Macromolecular Reaction Engineering*, vol. 9, n° 5, p. 522-529, 2015, doi: [10.1002/mren.201400065](https://doi.org/10.1002/mren.201400065).
- [7] A. W. Czanderna, F. J. Pern, « Encapsulation of PV modules using ethylene vinyl acetate copolymer as a pottant: A critical review », *Solar Energy Materials and Solar Cells*, p. 81, 1996.
- [8] A. Badiie *et al.*, « The thermo-mechanical degradation of ethylene vinyl acetate used as a solar panel adhesive and encapsulant », *International Journal of Adhesion and Adhesives*, vol. 68, p. 212-218, 2016, doi: [10.1016/j.ijadhadh.2016.03.008](https://doi.org/10.1016/j.ijadhadh.2016.03.008).
- [9] M. Narkis, J. Miltz, « Peroxide crosslinking of ethylene–vinyl acetate copolymer », *Journal of Applied Polymer Science*, vol. 21, n° 3, p. 703-709, 1977, doi: [10.1002/app.1977.070210311](https://doi.org/10.1002/app.1977.070210311).
- [10] B. K. Sharma *et al.*, « Effect of vinyl acetate content on the photovoltaic-encapsulation performance of ethylene vinyl acetate under accelerated ultra-violet aging », *Journal of Applied Polymer Science*, vol. 137, n° 2, 2020, doi: [10.1002/app.48268](https://doi.org/10.1002/app.48268).
- [11] A. P. Patel *et al.*, « Field-Aged Glass/Backsheet and Glass/Glass PV Modules: Encapsulant Degradation Comparison », *IEEE Journal of Photovoltaics*, vol. 10, n° 2, p. 607-615, 2020, doi: [10.1109/JPHOTOV.2019.2958516](https://doi.org/10.1109/JPHOTOV.2019.2958516).
- [12] A. Omazic *et al.*, « Relation between degradation of polymeric components in crystalline silicon PV module and climatic conditions: A literature review », *Solar Energy Materials and Solar Cells*, vol. 192, p. 123-133, 2019, doi: [10.1016/j.solmat.2018.12.027](https://doi.org/10.1016/j.solmat.2018.12.027).
- [13] N. S. Allen *et al.*, « Aspects of the thermal oxidation, yellowing and stabilisation of ethylene vinyl acetate copolymer », *Polymer Degradation and Stability*, vol. 71, n° 1, p. 1-14, 2000, doi: [10.1016/S0141-3910\(00\)00111-7](https://doi.org/10.1016/S0141-3910(00)00111-7).
- [14] A. Dadaniya, N. V. Datla, « Degradation prediction of encapsulant-glass adhesion in the photovoltaic module under outdoor and accelerated exposures », *Solar Energy*, vol. 208, p. 419-429, 2020, doi: [10.1016/j.solener.2020.08.016](https://doi.org/10.1016/j.solener.2020.08.016).
- [15] R. Meena *et al.*, « Comparative investigation and analysis of delaminated and discolored encapsulant degradation in crystalline silicon photovoltaic modules », *Solar Energy*, vol. 203, p. 114-122, 2020, doi: [10.1016/j.solener.2020.04.041](https://doi.org/10.1016/j.solener.2020.04.041).
- [16] L. Spinella *et al.*, « Chemical and mechanical interfacial degradation in bifacial glass/glass and glass/transparent backsheets photovoltaic modules », *Progress in Photovoltaics: Research and Applications*, vol. 30, n° 12, p. 1423-1432, 2022, doi: [10.1002/pip.3602](https://doi.org/10.1002/pip.3602).
- [17] G. Oreski *et al.*, « Properties and degradation behaviour of polyolefin encapsulants for photovoltaic modules », *Progress in Photovoltaics: Research and Applications*, vol. 28, n° 12, p. 1277-1288, 2020, doi: [10.1002/pip.3323](https://doi.org/10.1002/pip.3323).
- [18] S. Uličná *et al.*, « PV encapsulant formulations and stress test conditions influence dominant degradation mechanisms », *Solar Energy Materials and Solar Cells*, vol. 255, 2023, doi: [10.1016/j.solmat.2023.112319](https://doi.org/10.1016/j.solmat.2023.112319).
- [19] M. Baiamonte *et al.*, « Durability and Performance of Encapsulant Films for Bifacial Heterojunction Photovoltaic Modules », *Polymers*, vol. 14, n° 5, p. 1052, 2022, doi: [10.3390/polym14051052](https://doi.org/10.3390/polym14051052).
- [20] B. Adothu *et al.*, « UV resilient thermoplastic polyolefin encapsulant for photovoltaic module encapsulation », *Polymer Degradation and Stability*, vol. 201, 2022, doi: [10.1016/j.polymdegradstab.2022.109972](https://doi.org/10.1016/j.polymdegradstab.2022.109972).

- [21] B. Adothu *et al.*, « Newly developed thermoplastic polyolefin encapsulant—A potential candidate for crystalline silicon photovoltaic modules encapsulation », *Solar Energy*, vol. 194, p. 581-588, 2019, doi: [10.1016/j.solener.2019.11.018](https://doi.org/10.1016/j.solener.2019.11.018).
- [22] V. Chapuis *et al.*, « Compressive-shear adhesion characterization of polyvinyl-butyril and ethylene-vinyl acetate at different curing times before and after exposure to damp-heat conditions », *Progress in Photovoltaics: Research and Applications*, vol. 22, n° 4, p. 405-414, 2014, doi: [10.1002/pip.2270](https://doi.org/10.1002/pip.2270).
- [23] K. Nagayama *et al.*, « Influence of two-phase behavior of ethylene ionomers on diffusion of water », *Journal of Applied Polymer Science*, vol. 137, n° 31, 2020, doi: [10.1002/app.48929](https://doi.org/10.1002/app.48929).
- [24] J. Yang *et al.*, « Effect of various encapsulants for frameless glass to glass Cu(In,Ga)(Se,S)<sub>2</sub> photovoltaic module », *RSC Adv.*, vol. 5, n° 63, p. 51258-51262, 2015, doi: [10.1039/C5RA03663A](https://doi.org/10.1039/C5RA03663A).
- [25] Z. Yang *et al.*, « Novel EPE co-extruded encapsulating films with UV down-conversion power gain effect for highly efficient solar cells », *Solar Energy Materials and Solar Cells*, vol. 257, 2023, doi: [10.1016/j.solmat.2023.112373](https://doi.org/10.1016/j.solmat.2023.112373).
- [26] M. C. López-Escalante *et al.*, « Polyolefin as PID-resistant encapsulant material in PV modules », *Solar Energy Materials and Solar Cells*, vol. 144, p. 691-699, 2016, doi: [10.1016/j.solmat.2015.10.009](https://doi.org/10.1016/j.solmat.2015.10.009).
- [27] S. K. Chunduri, M. Schmela, « Market Survey Backsheets & Encapsulation 2022–2023 ».
- [28] M. Jaunich *et al.*, « Investigation of the curing state of ethylene/vinyl acetate copolymer (EVA) for photovoltaic applications by gel content determination, rheology, DSC and FTIR », *Polymer Testing*, vol. 52, p. 133-140, 2016, doi: [10.1016/j.polymertesting.2016.03.013](https://doi.org/10.1016/j.polymertesting.2016.03.013).
- [29] G. Oreski *et al.*, « Crosslinking and post-crosslinking of ethylene vinyl acetate in photovoltaic modules », *J. Appl. Polym. Sci.*, vol. 134, n° 23, 2017, doi: [10.1002/app.44912](https://doi.org/10.1002/app.44912).
- [30] Ch. Hirschl *et al.*, « Determination of the degree of ethylene vinyl acetate crosslinking via Soxhlet extraction: Gold standard or pitfall? », *Solar Energy Materials and Solar Cells*, vol. 143, p. 494-502, déc. 2015, doi: [10.1016/j.solmat.2015.07.043](https://doi.org/10.1016/j.solmat.2015.07.043).
- [31] S.-H. Schulze *et al.*, « Cure state assessment of EVA-copolymers for PV-applications comparing dynamic-mechanical, dielectric and calorimetric properties », *Solar Energy Materials and Solar Cells*, vol. 143, p. 411-417, 2015, doi: [10.1016/j.solmat.2015.07.024](https://doi.org/10.1016/j.solmat.2015.07.024).
- [32] G. M. Wallner *et al.*, « Comparison of Crosslinking Kinetics of UV-Transparent Ethylene-Vinyl Acetate Copolymer and Polyolefin Elastomer Encapsulants », *Polymers*, vol. 14, n° 7, Art. n° 7, 2022, doi: [10.3390/polym14071441](https://doi.org/10.3390/polym14071441).
- [33] W. Stark, M. Jaunich, « Investigation of Ethylene/Vinyl Acetate Copolymer (EVA) by thermal analysis DSC and DMA », *Polymer Testing*, vol. 30, n° 2, p. 236-242, 2011, doi: [10.1016/j.polymertesting.2010.12.003](https://doi.org/10.1016/j.polymertesting.2010.12.003).
- [34] Ch. Hirschl *et al.*, « Determining the degree of crosslinking of ethylene vinyl acetate photovoltaic module encapsulants—A comparative study », *Solar Energy Materials and Solar Cells*, vol. 116, p. 203-218, 2013, doi: [10.1016/j.solmat.2013.04.022](https://doi.org/10.1016/j.solmat.2013.04.022).
- [35] « LayTec - X Link for mass production ». <https://www.laytec.de/xlink-mass-production>.
- [36] « Standard Test Methods for Determination of Gel Content and Swell Ratio of Crosslinked Ethylene Plastics ». <https://www.astm.org/d2765-16.html>
- [37] « IEC 62788-1-6:2017: Measurement procedures for materials used in photovoltaic modules - Part 1-6: Encapsulants - Test methods for determining the degree of cure in Ethylene-Vinyl Acetate ». 2017. <https://webstore.iec.ch/publication/33050>
- [38] M. Hidalgo *et al.*, « A new DSC method for the quality control of PV modules: Simple and quick determination of the degree of crosslinking of EVA encapsulants », *Photovoltaics International*, vol. 14, p. 130-140, 2011.
- [39] P. Svoboda *et al.*, « Effect of octene content on peroxide crosslinking of ethylene-octene copolymers: Peroxide crosslinking of ethylene-octene copolymers », *Polym. Int.*, vol. 62, n° 2, p. 184-189, 2013, doi: [10.1002/pi.4277](https://doi.org/10.1002/pi.4277).

- [40] S. Ogier *et al.*, « A comparative study of calorimetric methods to determine the crosslinking degree of the ethylene-Co-vinyl acetate polymer used as a photovoltaic encapsulant », *Journal of Polymer Science Part B: Polymer Physics*, vol. 55, n° 11, p. 866-876, 2017, doi: [10.1002/polb.24335](https://doi.org/10.1002/polb.24335).
- [41] B. Lin *et al.*, « A polyolefin encapsulant material designed for photovoltaic modules: from perspectives of peel strength and transmittance », *J Therm Anal Calorim*, vol. 140, n° 5, p. 2259-2265, 2020, doi: [10.1007/s10973-019-09006-w](https://doi.org/10.1007/s10973-019-09006-w).
- [42] J. H. Park, S.-H. Hwang, « Construction and Characterization of Polyolefin Elastomer Blends with Chemically Modified Hydrocarbon Resin as a Photovoltaic Module Encapsulant », *Polymers*, vol. 14, n° 21, 2022, doi: [10.3390/polym14214620](https://doi.org/10.3390/polym14214620).
- [43] C. S. Sipaut, J. Dayou, « In situ FTIR analysis in determining possible chemical reactions for peroxide crosslinked LDPE in the presence of triallylcyanurate », *Funct. Compos. Struct.*, vol. 1, n° 2, 2019, doi: [10.1088/2631-6331/ab20c1](https://doi.org/10.1088/2631-6331/ab20c1).
- [44] V. Vacquea *et al.*, « Characterisation of the O-O peroxide bond by vibrational spectroscopy », 1997.
- [45] Z. Xia *et al.*, « A new method for measuring cross-link density in ethylene vinyl acetate-based encapsulant », *Photovoltaics International*, vol. 5, p. 150-159, 2009.